HAL
open science

# Correlation between the Indium Tin Oxide morphology and the performances of polymer light-emitting diodes

G. Wantz, L. Hirsch, N. Huby, L. Vignau, Jean-François Silvain, A. S. Barriére, J. P. Parneix

## To cite this version:

G. Wantz, L. Hirsch, N. Huby, L. Vignau, Jean-François Silvain, et al.. Correlation between the Indium Tin Oxide morphology and the performances of polymer light-emitting diodes. Thin Solid Films, 2005, 485 (1-2), pp.247-251. 10.1016/j.tsf.2005.03.022 . hal-00015487

**HAL Id: hal-00015487**

**https://hal.science/hal-00015487v1**

Submitted on 8 Dec 2005

**HAL** is a multi-disciplinary open access archive for the deposit and dissemination of scientific research documents, whether they are published or not. The documents may come from teaching and research institutions in France or abroad, or from public or private research centers.

L'archive ouverte pluridisciplinaire **HAL**, est destinée au dépôt et à la diffusion de documents scientifiques de niveau recherche, publiés ou non, émanant des établissements d'enseignement et de recherche français ou étrangers, des laboratoires publics ou privés.

# Correlation between the Indium Tin Oxide morphology and the performances of polymer light-emitting diodes

**Wantz G., Hirsch L., Huby N., Vignau L., Silvain J. F., Barriére A. S., Parneix J. P.**

**Abstract :**

This paper reports on performance enhancement of polymer light-emitting diodes (PLEDs) based on poly(2,5-bis(3′,7′-dimethyl-octyloxy)1,4-phenylene-vinylene) (BDMO-PPV) after Indium Tin Oxide (ITO) pre-treatment. Diluted *aqua regia* surface treatments of ITO substrates were investigated before PLEDs manufacturing. The correlation between ITO surface morphology and the properties of devices were discussed. The residual roughness, the global ITO thickness and developed anodic active area were found extremely dependent on treatment time. The performances of the ITO/BDMO-PPV/Ca/Al diodes were improved. With long treatments, the roughness was dramatically increased and poor PLEDs performances were achieved. The incorporation of a conducting polymer layer, poly(3,4-ethylene dioxythiophene) doped with polystyrene sulfonate, between the ITO layer and the emissive polymer, was also studied. With this buffer layer, no effect of the acidic treatment was observed on luminance–voltage characteristics and low turn-on voltage devices were made.

**Keywords :** Polymer light emitting diode; Indium tin oxide; Atomic force microscopy; Rutherford backscattering spectroscopy

## 1. Introduction

Polymer light-emitting diodes (PLEDs) have received worldwide enthusiastic attention due to their great potentials for low cost flat panel display applications. PLEDs are now likely to substitute liquid crystal displays in small hand-held electronic devices. However, a major disadvantage of PLEDs has to do with the instability under operating conditions and the lack of long-term reliability especially for large displays. In this sense, many device optimisations have been reported to improve lifetimes.

The basic structure of a PLED is very simple and includes a single electroluminescent layer (100 nm thick) sandwiched between a cathode and an anode. The performance of PLEDs is critically influenced by carrier injection into the emitting polymer [1] and [2]. Indium-tin oxide (ITO) is a common choice anode because it is conductive, transparent in the visible range and has a relatively high work function. But, without surface modification of the ITO, PLED devices usually exhibit poor performance. Many surface treatments of the ITO have been employed to improve the device performance, including *aqua regia* treatment [3], oxygen plasma treatment [4], [5], [6] and [7], atmospheric plasma treatment [8], ultra-violet ozone treatment [9], carbon tetrafluoride/oxygen treatment [10] and various coating treatments such as for example self-assembled monolayers [11] and [12]. Alternatively, by inserting an additional thin layer, such as copper-phtalocyanine [13], polyaniline [14], poly(3,4-ethylene dioxythiophene) doped with polystyrene sulfonate (PEDOT-PSS) [15] and [16], inorganic or organic insulators [17] and [18], emission intensity and device stability can be improved by lowering the driving voltage. The effects of such a buffer layer include the reduction of hole-injection energy barrier and the removal of contaminants from the ITO surface.

Our investigations deal with soft *aqua regia* treatments of the ITO and the use of PEDOT-PSS as a buffer layer. Their effects on polymer light-emitting device properties are exposed. Moreover, morphological studies of the anode are correlated with the performance enhancements due to the modification of the substrates.

Poly(phenylene-vinylene) (PPV) derivatives, for example poly(2-methoxy-5(2′-ethyl-hexoxy)1,4-phenylene-vinylene), have been extensively demonstrated as a promising light emitting polymer family in the past 10 years [19] and [20]. As a consequence, poly(2,5-bis(3′,7′-dimethyl-octyloxy)1,4-phenylene-vinylene), also known as $OC_{10}C_{10}$-PPV or BDMO-PPV, has been chosen as emissive polymer because of its high solubility and processability.

## 2. Experimental details

The diodes were fabricated using the following procedure. The ITO substrates on glass (from Merck Co.) underwent a wet cleaning procedure of successive 30 min ultrasonic baths in trichloroethylene,

ethanol and deionised water at room temperature. An acidic solution, based on hydrochloric acid and nitric acid in the following proportion $H_2O$ : HCl : $HNO_3$ 12 : 3 : 1, was used to treat the ITO. The substrates were treated at room temperature without stirring to promote the etching of roughness spikes rather than the etching of the global ITO thickness. Different treatment times were used: 5, 10, 15, 30 and 60 min. They were then abundantly rinsed with deionised water. In the first case, after blow drying, the BDMO-PPV, purchased from Aldrich, was deposited by spin-coating from a 15 g/L xylene solution at 1000 rpm in order to form a 175 nm thick layer. In the second case, a PEDOT-PSS (from Bayer, Baytron) film was spun, before the deposition of the BDMO-PPV layer, from a 3 wt.% water dispersion at 5000 rpm to form a 50 nm layer. This conducting polymer layer was cured at 80 °C under rotary pump vacuum for 1 h. Lastly, a calcium cathode was then thermally evaporated under vacuum (approximately $10^{-6}$ mbar) through a shadow mask. Finally, calcium (~ 40 nm thick) was capped with an aluminium layer (~ 150 nm thick) to minimize its oxidation. All devices investigated here had an active area of 10 $mm^2$. Samples were then stored and characterized under inert atmosphere (nitrogen glove box).

Surface morphology of ITO samples were examined by atomic force microscopy (AFM Veeco Dimension 3100). The thickness of the layers was evaluated with a profilometer (Temcor Alphastep).

Electrical sheet resistance of the ITO was measured using a Microworld four-point probe.

Rutherford Backscattering Spectroscopy (RBS) and Particle Induced X-ray Emission (PIXE) studies were performed using the 4 MeV Van de Graaff-type accelerator located at the Centre d'Etudes Nucléaires de Bordeaux Gradignan. Concerning RBS measurements, a 2 MeV $^4He^+$ incident beam was used with ($\Delta E_0 / E_0 = 10^{-4}$). The detection angle was $\theta_L = 155°$. The ionic current was set at about 0.5 nA. The samples were polarized at 200 V to trap the secondary electrons. The diameter of the $^4He^+$ incident beam is typically about 2 mm. A silicon surface barrier detector was used. It has a resolution of 13.5 keV, measured with $^{241}Am$, and solid angle $d\Omega$ = 2.8 msr, checked with a $Al_2O_3$/Al anodized thin film. Concerning the PIXE measurements, a 2.8 MeV $^1H^+$ incident beam was used. The ionic current was also set at 0.5 nA. A 315 µm thick carbon absorber was placed in front of a liquid nitrogen-cooled Canberra germanium detector, to enhance the signal of high energy photons. The detector resolution was guaranteed by the constructor at 160 eV. For both measurements, the signal was recorded via a low capacitance charge amplifier. The pressure during the experiments was about $10^{-7}$ mbar.

Contacts on PLEDs were taken using a Karl Suss prober. Devices were powered with a Keithley 2400 Sourcemeter. Light emission was retrieved using a monitored photodiode placed under the PLED. The received luminance and the efficiencies were then evaluated using the power response of the photoreceptor.

## 3. Results and discussion

### 3.1. Substrate characterization

The roughness of the ITO is often meant as a critical parameter for the performances of PLEDs. There are several different definitions of the terminology of surface roughness defined within the overall measuring length. $R_{pv}$ (peak-to-valley roughness) is the vertical distance between the highest and lowest points, $R_a$ (average roughness) is the arithmetic mean of the surface roughness profile from the centre line, $R_{r.m.s.}$ (root mean square roughness) is the root mean square value of the surface roughness from the centre line. It has been demonstrated that $R_{pv}$ is the relevant factor in terms of electrical instabilities of PLED and that a low average roughness $R_a$ is desirable [21].

Table 1 summarises the roughness data, the ITO thickness, deduced from the profilometer and RBS, and the sheet resistance as a function of the acidic treatment time of the ITO. Fig. 1 shows the AFM deduced topology of various samples. As received ITO substrates show a thickness of 115 nm and a topology consisting of a number of small and sharp peaks (Fig. 1a). After 5 min treatment, the global roughness significantly decreased due to the enhanced attack of the peaks rather than the wells leading to fewer sharp peaks (Fig. 1b). But, after longer treatments (30 and 60 min), the global roughness is extremely increased to reach larger values than for the untreated sample (Fig. 1c and d).

RBS and PIXE studies were performed on these samples to determine the reason of the roughness enhancement after intensive treatments. We show in Fig. 2(a), three RBS spectra corresponding to 0, 30 and 60 min of acidic treatment. For In and Sn, the energies of the backscattered $^4He^+$ particles

are theoretically 1.751 and 1.758 MeV respectively. As the resolution is 13.5 keV, In and Sn cannot be distinguished using this technique. Nevertheless, the reduction of the ITO thickness as a function of the acidic treatment time is clearly resolved with both, the reduction of the In/Sn peak width, and with the energy value of the glass substrate elements (Si, Ca and Na). The thickness values match those found by profilometry and are summarised in Table 1. Moreover, glass substrates elements are present at the surface of the sample which had been treated for 60 min. This indicates that the ITO layer does not cover the entire surface. By using the shape and the width of the Sn/In RBS peak in Fig. 2(a), we evaluated the thickness of the ITO spots on the glass substrate which range between 65 to 100 nm. From the decrease of the Sn/In RBS peak height, the surface occupied by ITO was estimated. We found that about 20% of the surface is free of ITO. A similar value is obtained considering the ratio of Si at the surface and Si under the ITO layer.

In the literature, it has been recently determined by X-ray photoemission spectroscopy (XPS) that these observed columnar formations can be interpreted as tin-oxide formations which is more hardly etched than indium-oxide by HCl-based wet treatments [22]. They support their conclusion by the fact that ITO is a double oxide made of tin-oxide and indium-oxide. Nevertheless, their conclusion is not consistent with our PIXE studies. Furthermore, as a consequence of the etching, the ITO thickness decreased and then the sheet resistance increased from 17.4 to 29.8 Ω. The intrinsic resistivity can be calculated from the sheet resistance by accounting for the ITO thickness. We obtained similar values among the samples around 1.9 ± 0.1 Ω μm which indicates that the composition of the ITO layer is not affected by the acidic treatment. Moreover, Li et al. [3] did not observe, by XPS, any chemical difference between *aqua regia*-treated and untreated ITO.

Actually, ITO is a polycrystalline single phase solid solution thin film with many grain boundaries. Contrary to the conclusion of Kim et al. [22], a preferential acidic attack on the ITO grain boundaries would be more consistent with our RBS, PIXE and AFM studies.

We also carried out a morphological study of PEDOT-PSS coated substrates. It appeared that a significant planarization of the ITO roughness is induced when adding PEDOT-PSS. For a 50 nm PEDOT-PSS coating (Fig. 1e and f), Table 1 shows a significant decrease of the roughness of the resulting anode between untreated ITO and on 60 min treated ITO. On Fig. 3 is plotted the increase of interface area implied by the acidic treatment where $S_r$ is the fully developed area and $S_p$ is the projected area of a selected square. It appeared that the anodic surface area is similar with a PEDOT-PSS layer whatever the ITO treatment time.

### 3.2. PLEDs characterization

The effect of the acidic treatment on electrical characteristics of devices is discussed in order to evaluate the effects of the roughness, as well as the use of PEDOT-PSS.

Fig. 4 shows the plot of the luminance as a function of the applied voltage for identical devices without PEDOT-PSS using a standard as received ITO and after different acidic treatment times. Values of luminance of thousands of candela per square meter were achieved. The treatment induced a significant increase of luminance (4000 Cd/m$^2$ at 13 V for a 30 min treatment vs. 850 Cd/m$^2$ at 13 V for untreated ITO). However, a longer treatment (60 min) did not exhibit higher performance (3300 Cd/m$^2$ at 13 V). For a treatment duration included between 0 and 30 min, the increase of specific anodic surface shown on Fig. 3 could be a reason of such luminance improvements. But, 10.8 mm$^2$ compared to 10.4 mm$^2$ is not consistent with observed luminance values. Another explanation could be an increase of the ITO work function due to the treatment but it has not been evaluated yet. The luminance decrease for treatment durations greater than 30 min can be explained by the reduction of the ITO / glass surface covering ratio as has been shown by the RBS study. We determined that for a 60 min acidic treatment, 20% of the surface is free of ITO which is consistent with the 17.5% luminance reduction. It corresponds to the reduction of the active anodic area.

The insertion of a PEDOT-PSS layer between ITO and BDMO-PPV exhibits smaller leakage currents but similar high field currents. Fig. 5 shows that no dependence of the luminance–voltage characteristics versus treatment time was observed with PEDOT-PSS and values of approximately 10,000 Cd/m$^2$ at 10 V were achieved. It is consistent with the results shown in Fig. 3 which indicates that the fully developed active areas of the anode are similar with PEDOT-PSS coating whatever the ITO treatment time.

The addition of a PEDOT-PSS interlayer induced a significant lowering of the turn-on voltage of the PLED. Performance enhancement by using a PEDOT-PSS interlayer cannot be only the result of the reduction of the surface roughness. We mentioned above that a similar roughness was found between 10 min-treated ITO and 50 nm PEDOT-PSS covered ITO. Moreover, PEDOT-PSS interlayer increases hole injection [15] and [16] by lowering the hole injection barrier. In addition, the PEDOT-PSS interlayer acts as a buffer layer between BDMO-PPV and ITO and avoids any chemical reaction between BDMO-PPV and ITO, which might possibly harm the correct operation of devices. Furthermore, indium diffusion from ITO to PPVs has been recently reported [23] and it is believed that PEDOT-PSS can also be a barrier to such detrimental diffusion.

Lifetime of PLED devices could be a pertinent parameter to evaluate the acidic treatment time effects. Nevertheless, in order to have reliable lifetime data for the *aqua regia* acidic treatment time, it has to be sure that the crucial parameter is the acidic treatment time and not the calcium and/or the PPV derivative oxidation. Thus, lifetime experiments have to be done either under inert atmosphere (glove box) or with a protective layer. As efficiency of the protective layer cannot be guaranteed, we are currently not able to present reliable lifetime data.

## 4. Conclusion

In this study, we have investigated by AFM, RBS and PIXE studies the role of acidic treatment on ITO substrates. After 5 and 10 min treatments, the global roughness significantly decreased due to the enhanced attack of the peaks rather than the wells leading to fewer sharp peaks. But, after longer treatments (30 and 60 min), the global roughness is extremely increased to reach larger values than for the untreated sample. We demonstrated that the chemical composition of the ITO layer has not been modified and the acidic attack mainly occurred at the boundary grains.

When a PEDOT-PSS interlayer was deposited, acidic treatment of ITO substrates did not influence neither the final fully developed active areas of the anode nor the PLEDs performances.

Finally, performances enhancement of PLEDs, by using a PEDOT-PSS interlayer, cannot be only the result of the reduction of the surface roughness. Hole injection enhancement and reduction of chemical interaction between ITO and BDMO-PPV have to be taken into account.

**Acknowledgements**

We gratefully acknowledge Serge Destor and Gilles Ruffié for their technical contributions in this study, and the CENBG team for their help in RBS and PIXE studies.

**References**

[1] R.N. Marks, D.D.C. Bradley, R.W. Jackson, P.L. Burn and A.B. Holmes, *Synth. Met.* **55–57** (1993), p. 4128.

[2] I.D. Parker, *J. Appl. Phys.* **75** (1994), p. 1656.

[3] F. Li, H. Tang, J. Shinar, O. Resto and S.Z. Weisz, *Appl. Phys. Lett.* **70** (1997), p. 2741.

[4] C.C. Wu, C.I. Wu, J.C. Sturn and A. Kahn, *Appl. Phys. Lett.* **70** (1997), p. 1348.

[5] K. Furukawa, Y. Terasaka, H. Ueda and M. Matsumura, *Synth. Met.* **91** (1997), p. 99.

[6] J.S. Kim, R.H. Friend and F. Cacialli, *Appl. Phys. Lett.* **74** (1999), p. 3084. [7] F. Zhu, *J. Soc. Inf. Disp.* **11** (2003), p. 605.

[8] I.-M. Chan, W.-C. Cheng and F.C.-N. Hong, *Appl. Phys. Lett.* **80** (2002), p. 13.

[9] S.K. So, W.K. Choi, C.H. Cheng, L.M. Leung and C.F. Kwong, *Appl. Phys., A* **68** (1999), p. 447.

[10] I.-M. Chan and F.C.-N. Hong, *Thin Solid Films* **444** (2003), p. 254.

[11] S.F.J. Appleyard and M.R. Willis, *Opt. Mater.* **9** (1998), p. 120.

[12] B. Choi, J. Rhee and H.H. Lee, *Appl. Phys. Lett.* **79** (2001), p. 2109.

[13] S.A. Vanslyke, C.H. Chen and C.W. Tang, *Appl. Phys. Lett.* (1996), p. 2160.

[14] S.A. Carter, M. Angelopoulos, S. Karg, P.J. Brock and J.C. Scott, *Appl. Phys. Lett.* **70** (1997), p. 2067.

[15] J.S. Kim, M. Granström, R.H. Friend, N. Johansson, W.R. Salaneck, R. Daik, W.J. Feast and F. Cacialli, *J. Appl. Phys.* **84** (1998), p. 6859.

[16] S.A. Carter, I. Grizzi, S.K. Heeks, D.J. Lacey, S.G. Latham, P.G. May, O.R. Delospanos, K. Pichler, C.R. Towns and H.F. Wittmanns, *Appl. Phys. Lett.* **71** (1997), p. 34.

[17] I.-M. Chan and F.C. Hong, *Thin Solid Films* **450** (2004), p. 304.

[18] L. Ke, R.S. Kumar, K. Zhang, S.J. Chua and A.T.S. Wee, *Synth. Met.* **140** (2004), p. 295.

[19] J.H. Burroughes, D.D.C. Bradley, A.R. Brown, R.N. Marks, K. Mackay, R.H. Friend, P.L. Burn and A.B. Holmes, *Nature* **347** (1990), p. 539. [20] A. Dodabalapur, *Solid State Commun.* **102** (1997), p. 259.

[21] Y.-H. Tak, K.-B. Kim, H.-G. Park, K.-H. Lee and J.-R. Lee, *Thin Solid Films* **411** (2002), p. 12.

[22] J.-S. Kim, F. Cacialli and R.H. Friend, *Thin Solid Films* **445** (2003), p. 358.

[23] M.J.M.d. Jong, D.P.L. Simons, M.A. Reijme, L.J.V. IJzendoorn, A.W.D.V.D. Gon, M.J.A.D. Voigt, H.H. Brongersma and R.W. Gymer, *Synth. Met.* **110** (2000), p. 1.

Table 1
Surface analysis data as a function of treatment times

| Anode | Thickness (nm) | Thickness (nm) | Sheet resistance (Ω/□) | Roughness (nm) | | |
|---|---|---|---|---|---|---|
| | Profilometer | RBS | | $R_a$ | $R_{r.m.s.}$ | $R_{pv}$ |
| ITO 0 min | 115 | 115 | 17.43 | 1.42 | 1.86 | 8.32 |
| ITO 5 min | 109 | 105 | 17.98 | 0.89 | 1.09 | 4.66 |
| ITO 15 min | 97 | 100 | 19.17 | 1.14 | 1.77 | 6.46 |
| ITO 30 min | 85 | 90 | 21.23 | 2.98 | 3.48 | 15.94 |
| ITO 60 min | 70 | 65–100 | 29.84 | 7.64 | 9.65 | 52.75 |
| ITO 0 min/ PEDOT-PSS | 115/60 | – | – | 0.63 | 0.85 | 4.15 |
| ITO 60 min/ PEDOT-PSS | 70/60 | – | – | 2.61 | 3.14 | 12.26 |

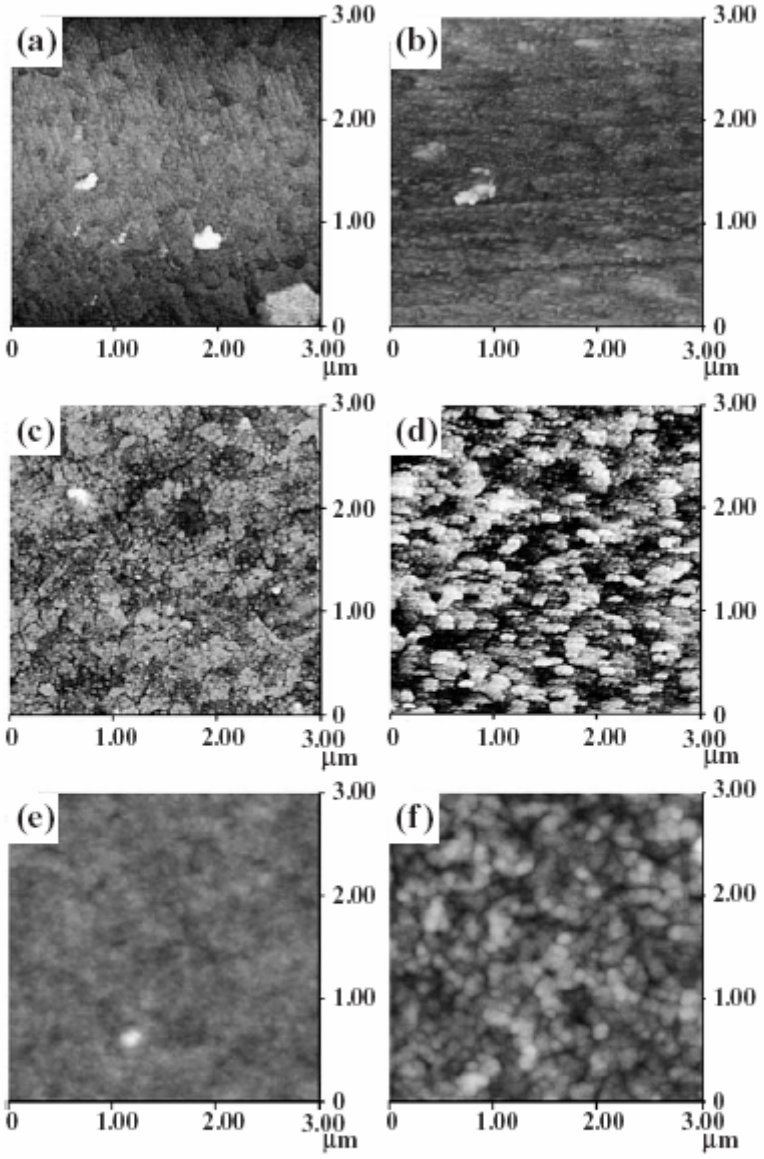


Fig. 1. AFM images: (a) ITO as received, (b) ITO after a 5 min treatment, (c) ITO after a 30 min treatment, (d) ITO after a 60 min treatment, (e) ITO as received covered with a 60 nm PEDOT-PSS layer, (f) ITO after a 60 min treatment covered with a 60 nm layer. The vertical scale is a black to white $z$-axis scale bar of 100 nm and the horizontal scale is 1 µm per division.

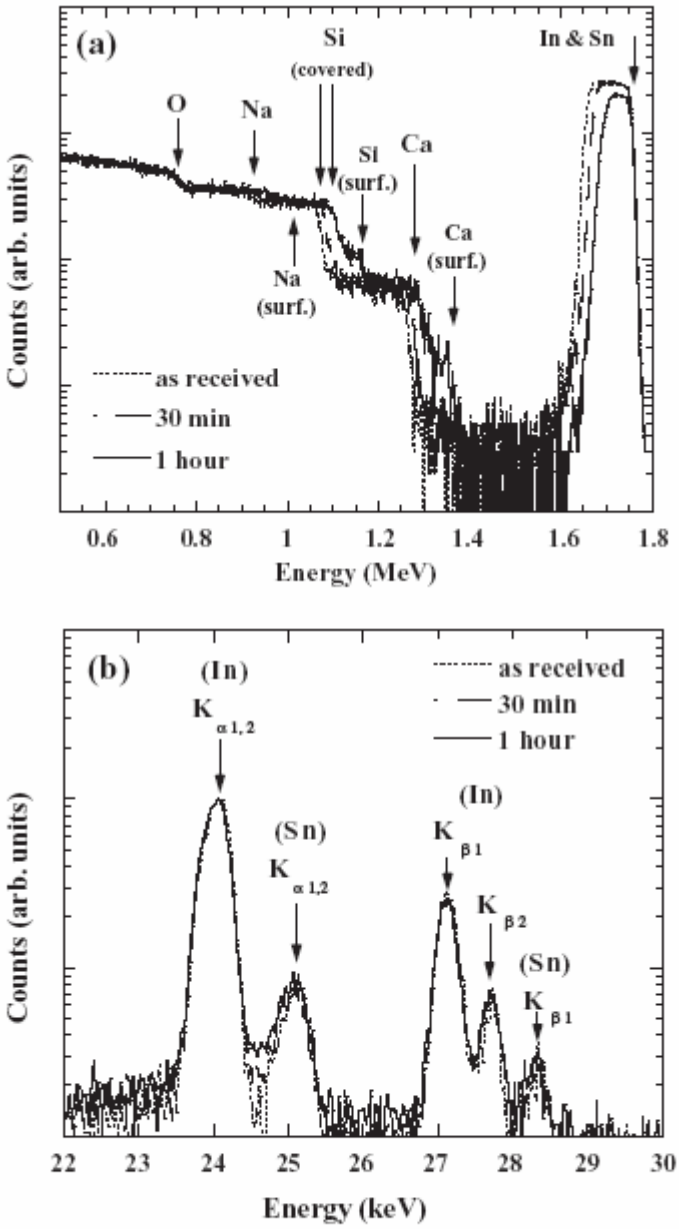


Fig. 2. RBS (a) and PIXE (b) spectra of ITO as received, ITO 30 min and ITO 60 min.

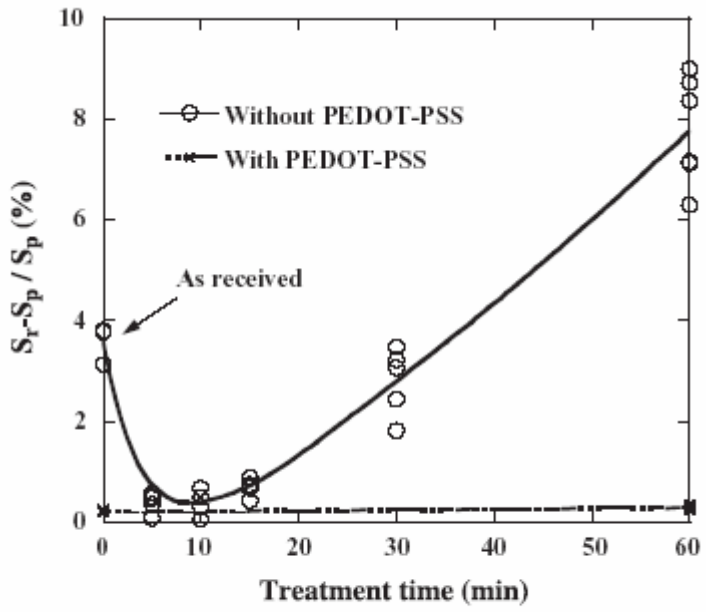


Fig. 3. Specific surface of the anode as a function of treatment time (with PEDOT-PSS in dashed line). $S_r$ and $S_p$ are respectively the real and projected surface.

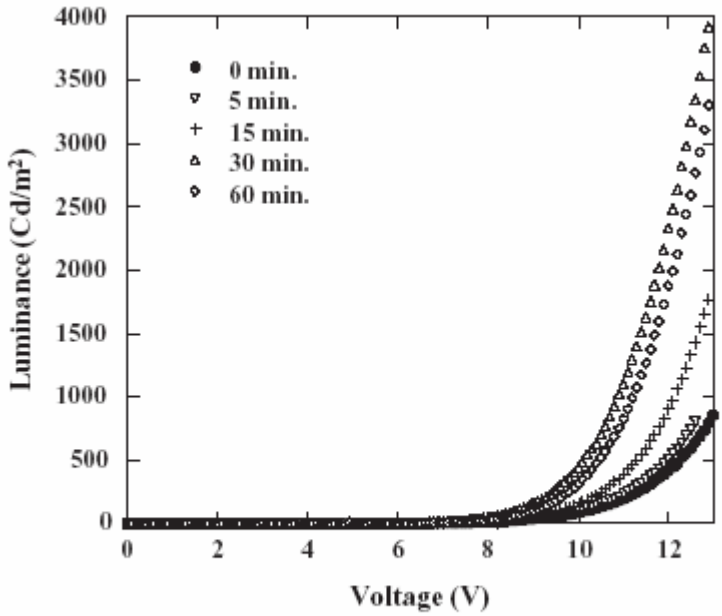


Fig. 4. Luminance vs. voltage characteristics of devices without PEDOT-PSS as a function of different acidic treatment times.

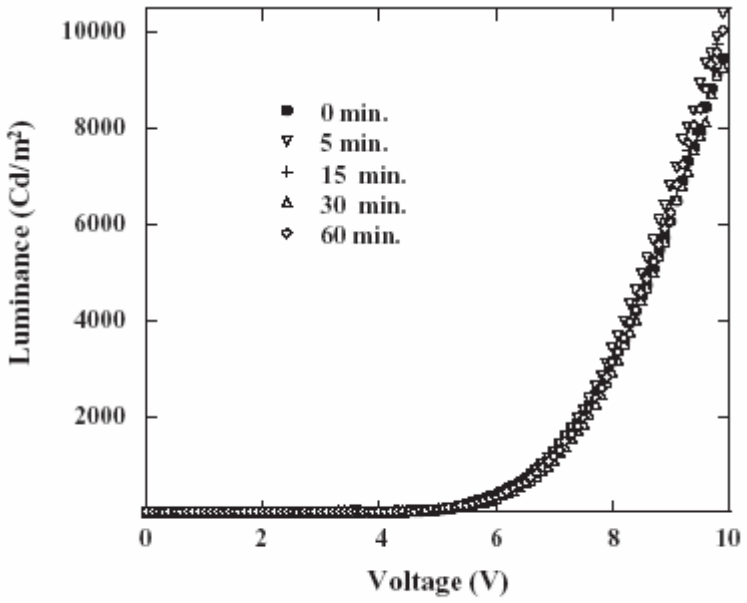


Fig. 5. Luminance vs. voltage characteristics of devices with PEDOT-PSS for a as received ITO substrate and after different acidic treatment times.